Conference materials
UDC 538.958 53.096
DOI: https://doi.org/10.18721/JPM.153.110

Investigation of temperature stability of germanium nanowires obtained by electrochemical deposition

D. L. Goroshko [1] ✉, E. A. Chusovitin [1], A. A. Dronov [2], I. M. Gavrilin [2]

[1] Institute of Automation and Control Processes Far Eastern Branch of the RAS, Vladivostok, Russia;
[2] National Research University of Electronic Technology, Moscow, Russia

✉ goroshko@iacp.dvo.ru

Abstract: The effect of vacuum annealing (600 °C, 30 min) on the temperature stability against oxidation in air of germanium nanowires obtained by cathodic deposition from aqueous solutions of germanium oxide was studied by the method of photoluminescence in the visible range and Raman scattering. The stability was checked by laser annealing at temperatures above 1000 °C. It was shown that the evolution of photoluminescence and Raman peaks is associated with the formation of germanium oxide or suboxide upon laser annealing. Preliminary vacuum annealing of the sample significantly suppresses this process. The observed effect is associated with the formation of germanium oxide and the influence of indium atoms on this process.

Keywords: germanium nanowires, germanium oxide, photoluminescence, Raman spectroscopy

Funding: This research was financially supported by the Russian Science Foundation (Project no. 20-19-00720).

Citation: Goroshko D. L., Chusovitin E. A., Dronov A. A., Gavrilin I.M., Investigation of temperature stability of germanium nanowires obtained by electrochemical deposition. St. Petersburg State Polytechnical University Journal. Physics and Mathematics. 15 (3.1) (2022) С. 59–64. DOI: https://doi.org/10.18721/JPM.153.110

Материалы конференции
УДК 538.958 53.096
DOI: https://doi.org/10.18721/JPM.153.110

Исследование температурной стабильности германиевых нанопроволок, полученных электрохимическим осаждением

Д. Л. Горошко [1] ✉, Е. А. Чусовитин [1], А. А. Дронов [2], И. М. Гаврилин [2]

[1] Институт автоматики и процессов управления Дальневосточного отделения РАН, г. Владивосток, Россия
[2] Национальный исследовательский университет «МИЭТ», г. Москва, Россия

✉ goroshko@iacp.dvo.ru

Аннотация. Методом фотолюминесценции в видимом диапазоне и КРС изучено влияние вакуумного отжига (600 °C, 30 мин) на температурную стабильность против окисления на воздухе нанопроволоки германия, полученные методом катодного осаждения из водных растворов оксида германия. Стабильность проверялась путем лазерного отжига при температуре более 1000 °C. Показано, что эволюция пиков фотолюминесценции и КРС связана с формированием оксида или субоксида германия при лазерном отжиге. Предварительный вакуумный отжиг образца существенно подавляет этот процесс. Наблюдаемый эффект связывается с особенностями формирования оксида германия и влиянием на этот процесс атомов индия.

Ключевые слова: германиевые нанопроволоки, оксид германия, фотолюминесценции, комбинационное рассеяние света

Финансирование: Работа выполнена при поддержке Российского научного фонда (проект № 20-19-00720).

Ссылка при цитировании: Горошко Д. Л., Чусовитин Е. А., Дронов А. А., Гаврилин И. М.

Исследование температурной стабильности германиевых нанопроволок, полученных электрохимическим осаждением // Научно-технические ведомости СПбГПУ. Физико-математические науки. 2022. Т. 15. № 3.1. С. 59–64. DOI: https://doi.org/10.18721/JPM.153.110

Introduction

Germanium nanowires (NWs) obtained by cathodic deposition from aqueous solutions of germanium oxide are a promising material for a new elemental base of electronic devices, since, compared to silicon, it has a higher charge carrier mobility, a smaller band gap, and a lower processing temperature [1]. Also of great interest is the use of Ge NWs in lithium-ion batteries [2–4]. In addition, they are an interesting example of nanosized structures in which quantum effects associated with size limitation can be observed [5, 6].

The possibility of electrochemical deposition of Ge NW from aqueous solutions using particles of low-melting metals (Ga, In, etc.) at nearly room temperature has been demonstrated [7, 8]. In this case, liquid metal nanodroplets have been used as an electrode for reduction of Ge-containing ions at the electrode surface, followed by dissolving and crystallizing the melt at the substrate interface. The growth mechanism, which is known as electrochemical liquid–liquid–solid (ec-LLS) crystal growth, is similar to the vapor–liquid–solid method [7].

It was shown in a series of works [9, 10] that successive laser annealing of Ge NWs obtained by this method lead to the recrystallization of samples and the appearance of Ge nanocrystals (NCs) of different sizes from 1.5 to 5 nm, and the behavior of the samples varies greatly depending on the presence or no vacuum annealing. In this paper, we analyze the effect of preliminary vacuum annealing of germanium nanowires obtained by cathodic deposition from aqueous solutions of germanium oxide on the change in their temperature stability against oxidation at high temperature at ambient conditions.

Materials and Methods

Electrochemical deposition of Ge NWs was carried out in a three-electrode cell. Fifty micrometer thickness titanium foil was used as the substrate. Indium nanoparticles were deposited on a Ti foil, as described in previous work [9]. The solution contained 0.05 M of germanium (IV) oxide GeO_2, 0.5 M of potassium sulfate K_2SO_4, and 0.5 M of succinic acid. Deposition was carried out at 0.2 $mA \cdot cm^{-2}$ at a solution temperature of 20 °C. The prepared samples were washed in deionized water and were dried in an argon flow. Some of the obtained samples were annealed at 600 °C in vacuum at a residual pressure below $1 \cdot 10^{-9}$ Torr for 30 min.

Photoluminescence (PL) measurements and backscattered Raman spectra were registered under excitation with focused laser radiation using a NTEGRA Spectra II micro-Raman spectrometer at room temperature and ambient conditions. We used a He-Ne laser (maximal power 50 mW and minimal spot diameter 2 μm) for Raman experiments. Photoluminescence spectra were registered under 405 nm excitation with background subtraction. The laser power was attenuated by means of neutral filters with different optical densities.

Before carrying out experiments on recording Raman and PL spectra, the maximum excitation power was determined, which did not lead to phase transformations in the sample, that would be reflected in changes in the spectra. However, to study the effect of high temperature on the state of the samples, exposure was carried out under a HeNe laser at maximum power for 1 – 60 seconds at ambient conditions. The temperature under the beam at such laser annealing was determined from the ratio of the intensities of the Stokes and anti-Stokes peaks of the optical phonon. Four sets of spectra were taken corresponding to different conditions of the sample. These sample conditions are conventionally presented in Table 1 and will be called accordingly.

Table 1

Sample list

Sample condition	Notation			
	A	B	C	D
Vacuum annealing	–	+	–	+
Laser annealing	–	–	+	+

Results and Discussion

PL was recorded in a wide wavelength range from 0.4 to 2 μm, where the appearance of exciton PL could be expected. The size effect in the samples under considered can lead to appearance of PL in the infrared range (IR), since the Bohr radius of a direct-gap exciton in Ge is 20–30 nm (depending on the conditions and calculation procedure [10], [11]) and can thus exceed the actually achievable size of a germanium nanocrystal or the filament diameter [9]. In this case, the emission of a photon with an energy of 1.3–2.67 eV is expected. Indeed, in a sample with Ge nanocrystals (NCs) 2–6 nm in size formed in a SiO_2 matrix, a weak shoulder with an energy of 1.6–1.8 eV was observed against the background of an intense peak with a position of 2.2–2.4 eV [10]. It should be noted that the intensity of this high-energy peak increased significantly upon annealing but the position did not change; nevertheless, the authors associated the nature of this PL with quantum-confinement effects in Ge NCs. Considering samples with Ge NCs less than 4 nm in size, the authors of [12] attributed the PL in the range of 2.2–2.3 eV to a new crystalline nanostructure in NCs with direct interband transitions; in this case, the absence of a temperature dependence of the position of the PL peak is not commented in any way. The convincing presence of IR PL in Ge nanowires was demonstrated in [13], however, as the authors point out, quantum confinement effects are unlikely to be involved in this, since the NW diameter is 40 nm and exceeds the exciton Bohr radius.

There was no photoluminescence for our samples with NWs in infrared region, but strong PL signal was found in the range of 400–950 nm (Fig. 1). The peak in the region of 450–475 nm in both spectra is associated with a drop in the detector sensitivity at the edge of the range; however, an increase in the intensity in the short-wavelength region below 500 nm is not an artifact of the measurements. It can be seen that in the initial state (without laser annealing, Fig. 1, *a*), a noticeable PL signal with a maximum at 635 nm is manifested only by the sample without vacuum annealing. Laser annealing of this sample for 1 second leads to a 4-fold increase in the PL intensity (Fig. 1, *b*, sample C) and a shift of the maximum to the blue region up to 536 nm. In turn, the PL intensity of the sample in the vacuum-annealed state B (Fig. 1, *a*) and D (Fig. 1, *b*) practically does not change: a slight elevated spectrum is observed in the region of 550–750 nm. A significant increase in the PL signal for sample D is achieved after laser annealing for 60 sec (Fig. 1, *b*); the peak maximum is located at about 600 nm.

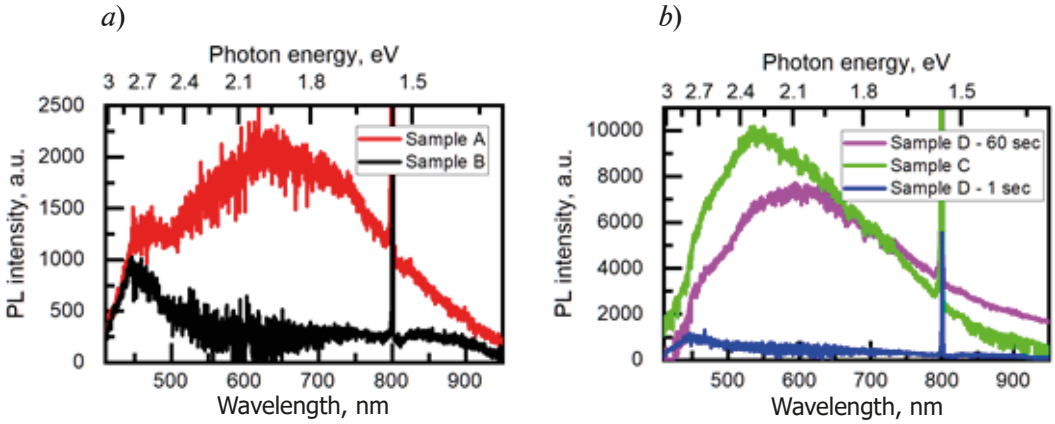

Fig. 1. PL spectra of sample with NWs before (*a*) and after (*b*) vacuum annealing. Different curves in each panel correspond to PL without and with laser annealing of different duration.
The sharp line at 800 nm is a second laser harmonic.

As shown above, the quantum size effect is an unlikely reason for the appearance of PL in a system with Ge NWs. Therefore, there must be other sources of PL observed in the studied samples. First of all, it can be germanium oxide, since germanium is actively oxidized at ambient conditions. The oxidation of germanium as the cause of PL is also indicated by its high intensity in the laser-annealed sample C. An estimate of the temperature in the region of the laser spot during annealing, measured from the ratio of Stokes and anti-Stokes peaks, gives a value of at least 1000 °C.

At present, most authors are inclined to believe that the source of PL in the visible and UV ranges is the Ge/GeO_x or GeO_x interface states. Similar conclusions are reached by studying freestanding Ge/GeO_2 core-shell NCs. Strong PL peaks in the same region are attributed to Ge/GeO_2 interface defect states [14] or GeO_xs [15]. Annealing in air or a hydrogen-containing atmosphere of nanocrystalline germanium obtained by chemical etching also allowed to conclude that the PL from these materials is from GeO_xs [16]. The effect of passivation on the PL from Ge NCs is shown in [17]. The deposition of a thin silicon layer on Ge NCs formed in high vacuum on the SiO_2 surface resulted in the appearance of a weak PL signal with a peak position of 0.85 and 0.82 eV, depending on the NC size. On the other hand, passivation reduced the PL intensity in the visible region due to the prevention of GeO_x formation on the surface.

The change in the state of germanium and its amount in the samples under the laser annealing is well traced in the Raman spectra (Fig. 2). After laser annealing of the sample without vacuum annealing (Fig. 2, *a*), the germanium phonon TO peak shifts from the position of 281 cm^{-1} to 300 cm^{-1}. In turn, the initial position of the TO peak in the vacuum annealed sample was 297.3 cm^{-1}, after laser annealing 300.7 cm^{-1}, and the intensity decreased by a factor of 4. Taking into account the fact that parts of the same sample were used for experiments with and without vacuum annealing, and the measurement conditions for all spectra in Fig. 2 coincided, it can be argued that, after laser annealing of the vacuum annealed sample, a significantly larger amount of germanium contained in NWs was retained in it. The shift of the Raman peaks to the blue region upon annealing is explained by an increase in the size of nanocrystalline grains in NWs. It is noteworthy that, prior to laser annealing, the position of the peak of the vacuum annealed sample is 297.3 cm^{-1}, which indicates recrystallization of NWs during the annealing.

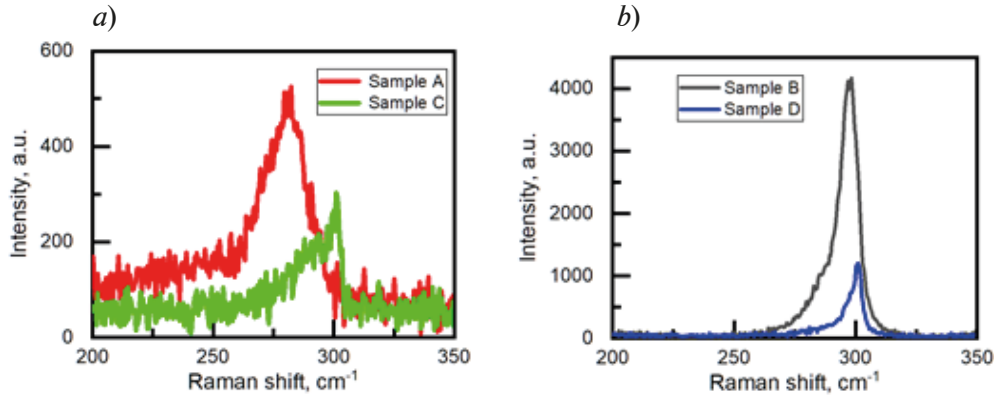

Fig. 2. Raman spectra of the sample with Ge NWs before (*a*) and after (*b*) vacuum annealing. Different curves in each panel correspond to the conditions without (samples A and B) and with (samples C and D) laser annealing.

It should be noted that the need for vacuum annealing in these samples was dictated by the need to get rid of the high concentration of indium used as a catalyst in the formation of NWs. According to our studies using in-situ electron beam annealing in a transmission electron microscope, indium segregates on the surface of the filaments. The results of studies in [18] indicate that the oxidation of germanium occurs at the GeO_2/Ge interface due to the decomposition of GeO_2. The resulting oxygen vacancy plays a key role in Ge oxidation, as oxygen atoms diffuse through these vacancies to interface with germanium with an exchange type of process. In turn, paper [19] presents a theoretical study of the influence of 4 and 3 valence metals on the passivation of vacancies in germanium suboxides in order to find out the reason for the success in obtaining excellent *p*- and *n*- MOSFET mobilities in the GeO_x/Al_2O_3 gate stack [20]. It turned out that the pre-existing oxygen vacancies in the intermediate GeO_2 layer affect the performance of the device. Since indium can exhibit 3 valence electrons in compounds, it can saturate oxygen vacancies in germanium suboxide by suppressing oxygen diffusion to the GeO_2/Ge interface and preventing oxidation. The difference between vacuum and laser annealing of NWs lies in the kinetics of these processes: vacuum annealing at 600 °C is not sufficient for the decomposition of GeO_2 [21], but this temperature is sufficient for active diffusion of indium.

Conclusion

Thus, the observed evolution of the PL spectra depending on the state of the sample is unambiguously related to oxidation of germanium NWs. A strong increase in PL after laser annealing at ambient conditions from a vacuum unannealed sample is explained by the formation of a large amount of oxide from germanium, which is included in NWs. This process correlates with the evolution of the Raman spectra, where the oxidation of NWs is accompanied by a significant decrease in the intensity of the TO phonon peak. After vacuum annealing, NWs become more resistant to oxidation, which manifests itself in the absence of PL in the studied range before laser annealing and its slight increase after a short laser annealing. In turn, the TO Raman peak remains quite intense. However, an increase in the duration promotes the occurrence of diffusion processes in NWs and their oxidation, which results in the appearance of intense PL. The analysis of these phenomena is based on the facts about the features of germanium oxidation, during which suboxides are formed, which, in turn, are the cause of PL in the studied range. Vacuum annealing leads to passivation of these germanium suboxides, resulting in a low PL intensity and resistance of NWs to oxidation at elevated temperatures.

Acknowledgments

This research was financially supported by the Russian Science Foundation (Project no. 20-19-00720).

REFERENCES

1. **Claeys C., Simoen E.,** Germanium-Based Technologies: From Materials to Devices, Elsevier, 2011.

2. **Liu S., Feng J., Bian X., Qian Y., Liu J., Xu H.,** Nanoporous germanium as high-capacity lithium-ion battery anode, Nano Energy. 13 (2015) 651–657.

3. **Tian H., Xin F., Wang X., He W., Han W.,** High capacity group-IV elements (Si, Ge, Sn) based anodes for lithium-ion batteries, Journal of Materiomics. 1 (2015) 153–169.

4. **Gavrilin I.M., Kudryashova Yu.O., Kuz'mina A.A., Kulova T.L., Skundin A.M., Emets V.V., Volkov R.L., Dronov A.A., Borgardt N.I., Gavrilov S.A.,** High-rate and low-temperature performance of germanium nanowires anode for lithium-ion batteries, Journal of Electroanalytical Chemistry. 888 (2021) 115209.

5. **Bruno M., Palummo M., Marini A., Del Sole R., Olevano V., Kholod A.N., Ossicini S.,** Excitons in germanium nanowires: Quantum confinement, orientation, and anisotropy effects within a first-principles approach, Phys. Rev. B. 72 (2005) 153310.

6. **Gu G., Burghard M., Kim G.T., Düsberg G.S., Chiu P.W., Krstic V., Roth S., Han W.Q.,** Growth and electrical transport of germanium nanowires, Journal of Applied Physics. 90 (2001) 5747–5751.

7. **Fahrenkrug E., Maldonado S.,** Electrochemical Liquid–Liquid–Solid (ec-LLS) Crystal Growth: A Low-Temperature Strategy for Covalent Semiconductor Crystal Growth, Acc. Chem. Res. 48 (2015) 1881–1890.

8. **Gavrilin I.M., Gromov D.G., Dronov A.A., Dubkov S.V., Volkov R.L., Trifonov A.Yu., Borgardt N.I., Gavrilov S.A.,** Effect of electrolyte temperature on the cathodic deposition of Ge nanowires on in and Sn particles in aqueous solutions, Semiconductors. 51 (2017) 1067–1071.

9. **Pavlikov A.V., Forsh P.A., Kashkarov P.K., Gavrilov S.A., Dronov A.A., Gavrilin I.M., Volkov R.L., Borgardt N.I., Bokova-Sirosh S.N., Obraztsova E.D.,** Investigation of the Stokes to anti-Stokes ratio for germanium nanowires obtained by electrochemical deposition, Journal of Raman Spectroscopy. 51 (2020) 596–601.

10. **Maeda Y.,** Visible photoluminescence from nanocrystallite Ge embedded in a glassy SiO_2 matrix: Evidence in support of the quantum-confinement mechanism, Phys. Rev. B. 51 (1995) 1658–1670.

11. **Kuo Y.-H., Li Y.-S.,** Variational calculation for the direct-gap exciton in the Ge quantum well systems, Phys. Rev. B. 79 (2009) 245328.

12. **Kanemitsu Y., Uto H., Masumoto Y., Maeda Y.,** On the origin of visible photoluminescence in nanometer-size Ge crystallites, Appl. Phys. Lett. 61 (1992) 2187–2189.

13. **Kawamura Y., Huang K.C.Y., Thombare S.V., Hu S., Gunji M., Ishikawa T.,** Brongersma M.L., Itoh K.M., McIntyre P.C., Direct-gap photoluminescence from germanium nanowires, Phys. Rev. B. 86 (2012) 035306.

14. **Giri P.K., Dhara S.,** Freestanding Core-Shell Nanocrystals with Varying Sizes and Shell Thicknesses: Microstructure and Photoluminescence Studies, Journal of Nanomaterials. 2012 (2012) 1–5.

15. **Kartopu G., Bayliss S.C., Hummel R.E., Ekinci Y.,** Simultaneous micro-Raman and photoluminescence study of spark-processed germanium: Report on the origin of the orange photoluminescence emission band, Journal of Applied Physics. 95 (2004) 3466–3472.

16. **Kartopu G., Bayliss S.C., Karavanskii V.A., Curry R.J., Turan R., Sapelkin A.V.,** On the origin of the 2.2–2.3 eV photoluminescence from chemically etched germanium, Journal of Luminescence. 101 (2003) 275–283.

17. **Aouassa M., Zrir M.A., Jadli I., Hassayoun L.S., Mghaieth R., Maaref H., Favre L., Ronda A., Berbezier I.,** Role of surface passivation on visible and infrared emission of Ge quantum dots formed by dewetting, Bull Mater Sci. 42 (2019) 69.

18. **Wang X., Nishimura T., Yajima T., Toriumi A.,** Thermal oxidation kinetics of germanium, Appl. Phys. Lett. 111 (2017) 052101.

19. **Golias E., Tsetseris L., Chroneos A., Dimoulas A.,** Interaction of metal impurities with native oxygen defects in GeO_2, Microelectronic Engineering. 104 (2013) 37–41.

20. **Zhang R., Huang P.-C., Lin J.-C., Takenaka M., Takagi S.,** Atomic layer-by-layer oxidation of Ge (100) and (111) surfaces by plasma post oxidation of Al_2O_3/Ge structures, Appl. Phys. Lett. 102 (2013) 081603.

21. **Laxman Shinde S., Kar Nanda K.,** Thermal oxidation strategy for the synthesis of phase-controlled GeO_2 and photoluminescence characterization, CrystEngComm. 15 (2013) 1043–1046.

THE AUTHORS

GOROSHKO Dmitry L.
goroshko@iacp.dvo.ru
ORCID: 0000-0002-1250-3372

DRONOV Alexey A.
noiz@mail.ru
ORCID: 0000-0001-6085-2481

CHUSOVITIN Evgeny A.
eliot@list.ru
ORCID: 0000-0002-8162-5533

GAVRILIN Ilya M.
gavrilin.ilya@gmail.com
ORCID: 0000-0002-0278-1598

Received 31.05.2022. Approved after reviewing 07.07.2022. Accepted 08.07.2022.